Stem Cell Reports
Article

ISSCR

OPEN ACCESS

Telomerase Protects Werner Syndrome Lineage-Specific Stem Cells from Premature Aging

Hoi-Hung Cheung,[1,2,*] Xiaozhuo Liu,[1,2] Lucile Canterel-Thouennon,[1] Lu Li,[2] Catherine Edmonson,[1] and Owen M. Rennert[1,*]

[1]Laboratory of Clinical and Developmental Genomics, Eunice Kennedy Shriver National Institute of Child Health and Human Development, National Institutes of Health, Bethesda, MD 20892, USA

[2]School of Biomedical Sciences, Faculty of Medicine, the Chinese University of Hong Kong, Shatin, N.T., 852 Hong Kong S.A.R.

*Correspondence: cheunghh@cuhk.edu.hk (H.-H.C.), rennerto@mail.nih.gov (O.M.R.)

http://dx.doi.org/10.1016/j.stemcr.2014.02.006

SUMMARY

Werner syndrome (WS) patients exhibit premature aging predominantly in mesenchyme-derived tissues, but not in neural lineages, a consequence of telomere dysfunction and accelerated senescence. The cause of this lineage-specific aging remains unknown. Here, we document that reprogramming of WS fibroblasts to pluripotency elongated telomere length and prevented telomere dysfunction. To obtain mechanistic insight into the origin of tissue-specific aging, we differentiated iPSCs to mesenchymal stem cells (MSCs) and neural stem/progenitor cells (NPCs). We observed recurrence of premature senescence associated with accelerated telomere attrition and defective synthesis of the lagging strand telomeres in MSCs, but not in NPCs. We postulate this "aging" discrepancy is regulated by telomerase. Expression of hTERT or p53 knockdown ameliorated the accelerated aging phenotypein MSC, whereas inhibition of telomerase sensitized NPCs to DNA damage. Our findings unveil a role for telomerase in the protection of accelerated aging in a specific lineage of stem cells.

INTRODUCTION

Patients with Werner syndrome (WS) exhibit premature aging and early onset of a cancer during adulthood (third to fourth decade) (Chen and Oshima, 2002; Muftuoglu et al., 2008). Autosomal recessive mutations of the RecQ helicase *WRN* are commonly found in the majority of WS patients, although non-WRN mutations have been documented (Chen et al., 2003).

WRN is a critical protein for DNA replication, repair, recombination, and telomere maintenance (Crabbe et al., 2004; Opresko et al., 2004). An important molecular event seen in WS pathology is dysfunction of telomeres. It results in accelerated telomere attrition and failure to fully synthesize the lagging strand sister telomeres (Brosh et al., 2001; Crabbe et al., 2004). Critically short telomeres have been known to elicit a DNA damage response and trigger cellular senescence (Abdallah et al., 2009; d'Adda di Fagagna et al., 2003; Takai et al., 2003). Another observed phenotype in WS cells is genome instability, perhaps due to deficient DNA repair and uncapping of chromosome ends. WRN is known to interact with a number of proteins involved in DNA repair, recombination, and telomere protection (Crabbe et al., 2007; Laud et al., 2005; Li and Comai, 2001). These biological functions and molecular mechanisms of WRN serve as the basis for our understanding of the clinical pathology of accelerated aging (Rossi et al., 2010). A fascinating clinical feature of WS is the predominant aging that fibroblasts and mesenchymal tissues exhibit (Chen and Oshima, 2002; Goto et al., 2013). Although the spectrum of the aging disorder in many aspects resembles natural aging (such as graying hair, cataract, osteoporosis, and atherosclerosis), neurodegeneration, such as that which occurs in Alzheimer and Parkinson diseases, is seemingly not associated with WS (Goto et al., 2013; Mori et al., 2003). These observations suggest WS is not simply an accelerated aging phenomenon, such as that observed in normally aged people; however, the reason for this selectively accelerated aging remains unclear.

We reasoned that lineage-specific aging in WS patients is a consequence of factor(s) that control aging of stem cells. It gradually develops into diverse clinical presentations, reflecting the heterogeneity seen in different tissues. To experimentally query this phenomenon, we generated patient-specific induced pluripotent stem cells (iPSCs) and differentiated them to mesenchymal stem cells (MSCs) and neural progenitor cells (NPCs) to study the cellular aging phenotype. We identified telomerase as a critical factor in controlling premature senescence in specific lineages of stem cells.

RESULTS

Reprogramming Prevents Cellular Aging in WS Fibroblasts

As a consequence of WRN deficiency, WS skin-cultured fibroblasts divide slowly and rapidly become senescent, a characteristic of premature aging (Figures S1A and S1B available online). Senescence and genomic instability are

barriers for somatic cell reprogramming (Banito et al., 2009). Despite these barriers, we successfully reprogrammed WS fibroblasts using efficient polycistronic lentivirus in combination with inhibitors that target the TGF-β pathway and the epigenetic modifier HDAC. Four WS fibroblasts cultures, including a line from a non-classic WS that expresses wild-type WRN (AG06300), were successfully reprogrammed to iPSCs (Table S1). These WS iPSCs were maintained in culture for more than 35 passages without changes in their morphology. WS iPSCs expressed pluripotency markers and showed characteristics of human embryonic stem cells (hESCs), including the stringent teratoma formation assay in SCID mice (Figures S1C–S1E). BrdU incorporation indicated that WS iPSCs synthesized DNA at a slightly slower rate than normal iPSCs; however, the difference was statistically insignificant ($p = 0.09$, t test; Figure S1F). We compared gene expression profiles before and after reprogramming. More than 800 genes were differentially expressed in the parental fibroblasts (fold change >2 or <−2; $p < 0.05$; one-way ANOVA); most were involved in cellular aging (Figures 1A and 1B). Surprisingly, after reprogramming, nearly all of the fibroblast differentially expressed genes (99.7%) were erased in the derived iPSCs. The transcriptome of reprogrammed WS iPSCs were highly similar to normal iPSCs (Figure 1C). Unsupervised whole-genome clustering demonstrated the WS iPSC transcriptome was indistinguishable from normal iPSCs, indicating that reprogramming has reset the aging phenotype.

Restoration of Telomere Function in WS iPSCs

WRN mutant cells display critically short telomeres and defective synthesis in the lagging strand of sister telomeres, leading to premature senescence (Crabbe et al., 2004; Ishikawa et al., 2011; Schulz et al., 1996). Previous studies demonstrated that telomerase overexpression prevents the expression of the telomere defect in WS fibroblasts (Crabbe et al., 2007). As expected, following reprogramming, WS iPSCs showed little deficit of telomere synthesis as revealed by telomere chromosome-orientation fluorescence in situ hybridization (CO-FISH). Most of the cells could successfully synthesize the lagging strands of their telomeres despite the lack of WRN protein (Figure 2A). Normal telomere function in reprogrammed WS cells is further supported by successful reactivation of telomerase and expression of telomerase complex genes (*TERT*, *TERC*, and *DKC1*) (Figures 2B and S2A). The telomere length of WS iPSCs was elongated to a similar extent as that observed in normal iPSCs or hESCs (Figure 2C). Moreover, genes that maintain telomere stability (shelterin) were expressed at a level similar to that observed in normal iPSCs (Figure S2B). These observations indicate at pluripotency WS cells have corrected their telomere-associated defects.

Recurrence of Premature Senescence and Telomere Dysfunction in Differentiated MSCs

Our observations on WS iPSCs telomere function do not provide a rationale for the premature aging phenotype observed in affected tissues of patients' mesenchymal lineages, such as bone, vascular cells, dermis, and hair (Chen and Oshima, 2002; Muftuoglu et al., 2008). We postulated that in WS, because the premature aging phenotype is predominantly expressed in mesenchymal lineages as a consequence of premature senescence, MSC exhaustion may occur at an early age. To model cellular aging of MSCs, we differentiated iPSCs to MSCs using a previously reported protocol (Lian et al., 2010). Both normal and WS iPSC-derived MSCs expressed positive and negative surface markers similar to that observed in human bone marrow-derived MSCs (BM-MSCs) (Figures S3A and S3B). The iPSC-derived MSCs exhibited multipotency and differentiated to fat, bone, and cartilage-like cells in specific induction media (Figure S3C). Unlike hESCs/iPSCs, MSCs have a limited replicative potential due to an end replication problem (Lu et al., 2013). Comparison of the proliferation capacity of these cells revealed slower cell proliferation and early entry to senescence of the WS MSCs (Figures 3A–3C). Premature senescent WS MSCs expressed more p53 and the senescence markers p21 (also known as CDKN1A) and p16 (also known as CDKN2A) (Figure 3D). In late passage, WS MSCs had shortened telomere length, an evidence of accelerated telomere erosion (Figure 3E). BrdU incorporation experiments indicated a smaller fraction of cells in S phase for WS MSCs; however, the difference of BrdU incorporation in iPSCs was marginal and insignificant (Figures 3F and S1F). CO-FISH telomere analysis revealed a high incidence of sister telomere loss in the lagging strand (Figures 3G and 3H). These results are consistent with the previously reported observation in WS fibroblasts or WRN-depleted cells (Crabbe et al., 2004). The premature senescence and defective synthesis of the lagging strand telomeres in derived MSCs recapitulated that observed in WS fibroblasts.

Rescue of Premature Senescence by hTERT or p53 Depletion

We speculate the slow cell proliferation and accelerated senescence found in WS MSCs is due to the downregulation of telomerase activity, which sensitizes cells to DNA/telomere replication in a WRN-deficient background. To test this hypothesis we generated hTERT-knockin WS fibroblasts and subsequently reprogrammed them to pluripotency. These genetically modified iPSCs showed similar expression profiles and telomerase reactivation to that observed in unmodified WS iPSCs (Figure S4A). Upon differentiation to MSCs (WS-MSC_{tert}), telomerase activity remained high compared to those derived from

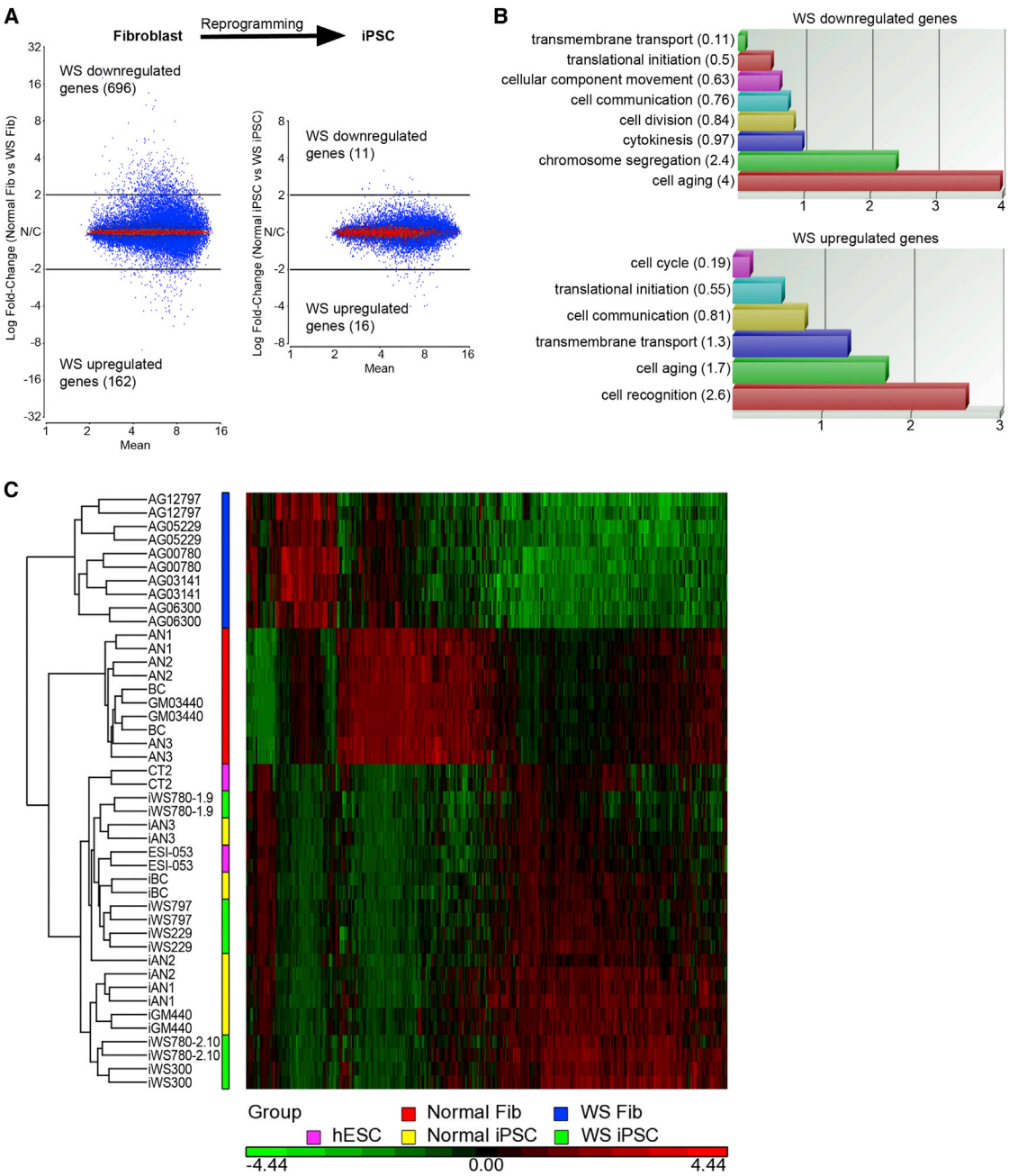

Figure 1. Reprogramming to Pluripotency Prevents Premature Senescent Phenotype in WS Fibroblasts

(A) Expression microarray analysis comparing the number of differentially expressed genes (fold change > 2; FDR < 0.05) between normal and WS cells before (fibroblasts) and after reprogramming (iPSCs). Reprogramming reduces the number of differentially expressed transcripts from 858 to 27.

(B) Gene ontology analysis for the differentially expressed genes in WS fibroblasts based on the cellular process of biological function. The major categories of the differentially expressed genes are cell aging and cell recognition.

(C) Unsupervised hierarchical clustering for fibroblast and iPSC samples based on the differentially expressed genes identified in WS fibroblasts. Two hESC lines CT2 and ESI-053 are included.

See also Figure S1.

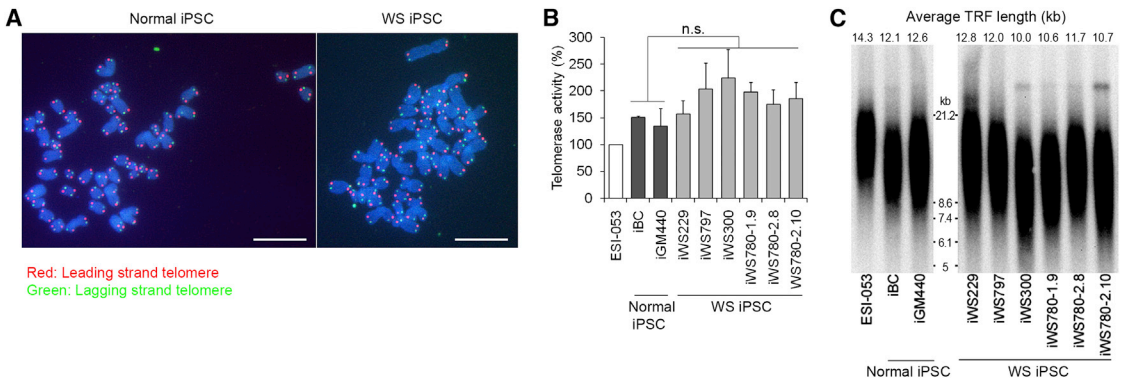

Figure 2. Restoration of Telomere Function in Reprogrammed WS iPSCs

(A) Normal synthesis of both the leading and the lagging strand sister telomeres in WS iPSCs by chromosome orientation fluorescence in situ hybridization (CO-FISH).

(B) Reactivation of telomerase activity in WS iPSCs by telomeric repeat amplification protocol (TRAP). Values represent mean of technical replicates ± SD (n = 3).

(C) Telomere length in WS iPSCs by Southern blot of terminal restriction fragment (TRF). The differences of telomerase activity and TRF length between normal and WS iPSCs are not significant (n.s.). Scale bar, 10 μm.

See also Figure S2.

unmodified WS-MSCs (Figure S4B). There was no evidence of retroviral gene silencing upon differentiation because WS-MSC$_{tert}$ expressed similar telomerase activity to hTERT-knockin WS fibroblasts. These cells remain antibiotic resistant, indicative of a lack of silencing of the retroviral vector. WS-MSC$_{tert}$ showed a higher proliferation rate and improved replicative potential with reduced senescence despite the absence of WRN protein (Figures 4A, 4C, and 4D). This hTERT-ameliorated effect was reversed by prolonged treatment with the telomerase inhibitor BIBR 1532 (Figures S4C and S4D). To understand how telomerase activity rescues premature aging in WS MSCs, we examined the expression of the senescence markers p21 and p16, activation of DNA double strand breaks (p-ATM) and the presence of DNA damage markers (53BP1 and γH2AX) in normoxia or oxidative stress induced by hydrogen peroxide. WS-MSC$_{tert}$ expressed higher p53 and p21 (a target of p53), perhaps because of the stabilization of p53 by telomeric repeats (Milyavsky et al., 2001). Nevertheless, activation of p53 was not increased in WS-MSC$_{tert}$ despite the higher basal level (Figure S4I). Another senescence marker p16, as expected, was decreased in WS-MSC$_{tert}$. When WS MSCs were exposed to H_2O_2, 53BP1 was activated at low oxidative stress (50 μM), whereas γH2AX was induced at high oxidative stress (250 μM) accompanied by activation of ATM (p-ATM) (Figure S4E). The expression of hTERT in WS MSCs appears to rescue senescence through reduction of the p16 level (but not of p53/p21) and the DNA damage marker γH2AX. These data support the critical role of telomerase in cell proliferation and the cell's replicative potential, as well as in preventing DNA damage and premature senescence in WRN-deficient cells. We suggest that, without protection of the telomere by telomerase, WS cells quickly enter senescence via the p53 pathway. To verify this postulation, we derived stable p53 knockdown cells by RNAi (p53i) in WS fibroblasts. When these p53i WS cells were reprogrammed to iPSCs, they showed little difference from unmodified iPSCs; however genomic instability was present (Table S2). Genomic instability due to p53 depletion in iPSCs has been previously reported (Kawamura et al., 2009; Marión et al., 2009a). Upon differentiation to MSCs (WS-MSC$_{p53i}$), p53 protein remains low, evidence of persistent expression of p53 shRNA (Figure S4F). As a consequence in MSCs, p53i enhanced their proliferative potential and rescued the premature senescence phenotype without the need for high telomerase activity and long telomere length (Figures 4B–4D). As expected, WS-MSC$_{p53i}$ expressed less p21 and phosphorylated p53 (Figure S4G). Next, we examined the telomere status in these genetically modified cells. Longer telomere length was found in WS-MSC$_{tert}$, but not in WS-MSC$_{p53i}$, suggesting a rescue of the accelerated telomere attrition by telomerase (Figure 4E). CO-FISH analysis revealed a reduction of defective synthesis for the lagging strand telomeres in WS-MSC$_{tert}$, but not in WS-MSC$_{p53i}$ (Figures 4F and 4G). Collectively, these data support the critical role of telomerase in preventing premature senescence in MSCs by restoring telomere function. p53 appears to be a downstream effector because a similar effect was achieved as a consequence of depleting p53 and bypassing the senescence pathway.

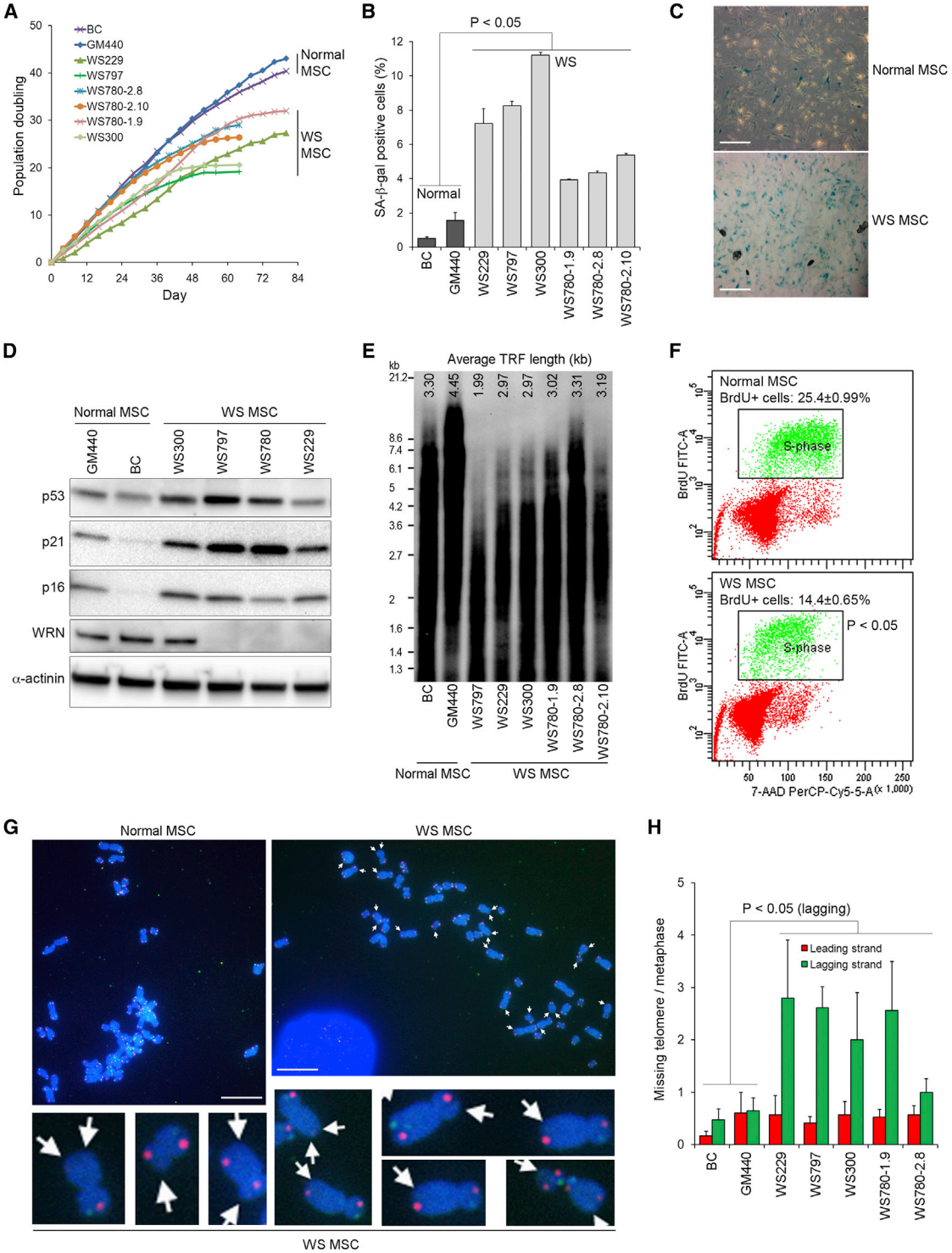

Figure 3. Recurrence of Premature Senescence and Telomere Dysfunction in WS MSCs

(A) Reduced cell proliferation and replication potential in WS MSCs with continuous culture for 76 days.

(B) Quantitative analysis for percentage of senescent cells in MSCs after 44 days of culture (p11). A significant difference is found between normal and WS MSCs ($p < 0.05$).Values represent mean of technical replicates ± SD ($n = 3$).

(C) Representative images for normal and WS MSCs by SA-β-galactosidase staining.

(legend continued on next page)

Telomerase Activity in NPCs and Its Role in Protecting DNA Damage

Because telomerase has a critical function in protection of telomere erosion in MSCs, we speculate that the neural lineage telomerase is differentially regulated and protects neural lineage cells from accelerated senescence. To test this hypothesis, we differentiated iPSCs to NPCs (Figure S5A). The derived cells expressed NPC markers NESTIN and SOX1 and were able to differentiate them to neurons and astrocytes in neuronal induction media (Figure S5B). As expected, WRN protein was expressed in both normal NPCs and MSCs but was undetectable in WRN mutant WS lines (Figure S5C). We measured telomerase activity and telomere length in NPCs. A telomeric repeat amplification protocol (TRAP) assay showed a higher telomerase activity in NPCs than in MSCs, although the level was lower than pluripotent hESCs/iPSCs. To our surprise, the telomerase activity of normal and WS NPCs was not significantly different ($p = 0.78$, t test; Figure 5A). Similarly the telomere length observed in WS NPCs was comparable to normal NPCs (Figure 5B). CO-FISH analysis revealed a low incidence of missing sister telomeres in the lagging strands indicative of normal telomere synthesis during replication (Figure 5C). WS NPCs divided actively in culture and incorporated BrdU at a rate similar to normal NPCs (Figures 5D and S5D). No apparent premature senescence was observed in NPC cultures. Our observations suggest relatively normal cellular proliferation and telomere function in NPCs, consistent with the clinical phenotype of WS (Goto et al., 2013). Because telomerase is expressed in NPCs, and ectopic expression of hTERT in MSCs is able to rescue premature senescence in the absence of WRN (Figure 4), we tested whether telomerase inhibition in WS NPCs sensitizes cells to accelerated aging. Senescence-associated (SA)-β-galactosidase activity was not detected upon 3 days of treatment with the telomerase inhibitor BIBR 1532. We speculate that the long telomere reserves in NPCs may prevent these cells from senescence (Taboski et al., 2012). However, analysis of the DNA damage marker γH2AX indicated a telomerase-sensitive response. BIBR 1532 sensitized WS NPCs to γH2AX, a chromatin marker induced by replicative stress or DNA damage. All WS lines showed a remarkable increase of γH2AX; however, the change in BrdU incorporation (an indication of mitotic arrest) and NESTIN expression (an indication of undifferentiated state for NPCs) did not differ between normal and WS cells (Figure 5E). A longer inhibition of telomerase for 6–8 days slowed their proliferative capacity; this phenomenon was more prominent in WS NPCs (Figure S5E). However, inhibition of telomerase in WS NPCs decreased the p53 level and its target p21, whereas p16 was not detectable (Figure S5F).The consequent change in the p53 level in WS NPC survival remains to be addressed in future studies. In summary, our data suggest that telomerase benefits cell growth and prevents premature aging or DNA damage by correcting telomere function in a specific lineage of WS stem/progenitor cells; it is more severely compromised in MSCs and to a lesser extent in NPCs and iPSCs.

DISCUSSION

Our data demonstrate premature senescence caused by WRN loss can be reversed by nuclear reprogramming, possibly as a consequence of reactivation of telomerase machinery that corrects the telomere defect. Reprogramming of normally aged fibroblasts or diseases of laminopathies and Hutchinson-Gilford Progeria syndrome have been reported (Lapasset et al., 2011; Liu et al., 2011; Zhang et al., 2011). Our observations highlight telomere function in WS cells, because abnormal telomere homeostasis is a critical molecular event in WS pathology (Chang et al., 2004; Crabbe et al., 2004; Ishikawa et al., 2011; Laud et al., 2005; Multani and Chang, 2007). Telomere length in pluripotent WS cells appears to be normal. With differentiation premature senescence recurs, and aberrant telomere synthesis is found in derived MSCs, but not in NPCs, indicative of a lineage-specific aging phenomenon. This observation is consistent with the clinical phenotype of WS, where mesenchymal tissues are severely affected but mild or no symptoms are associated with neural lineages (Goto et al., 2013). The inability to perform systematic studies of different cell types or tissues during embryonic development and in adulthood validates iPSC technology as a valuable tool to study its pathogenesis. By comparing the different stem/progenitor cells, we identified a dramatic difference in telomerase activity. In line with other studies,

(D) Expression of p53 and senescence markers p21 and p16 proteins by Western blot analysis. WS MSCs express more proteins of p53, p21, and p16.
(E) Accelerated telomere attrition at late passage (p17) of WS MSCs as revealed by TRF Southern blot.
(F) BrdU incorporation between normal and WS MSCs. The difference is significantly different ($p < 0.05$).
(G) Increased incidence of defective synthesis for the lagging strand telomeres by CO-FISH. Arrows indicate the missing telomeres at metaphase.
(H) Quantification of (F). Values represent mean ± SEM (at least 15 metaphase cells were analyzed).
Scale bar, 100 μm (C) or 10 μm (G). See also Figure S3.

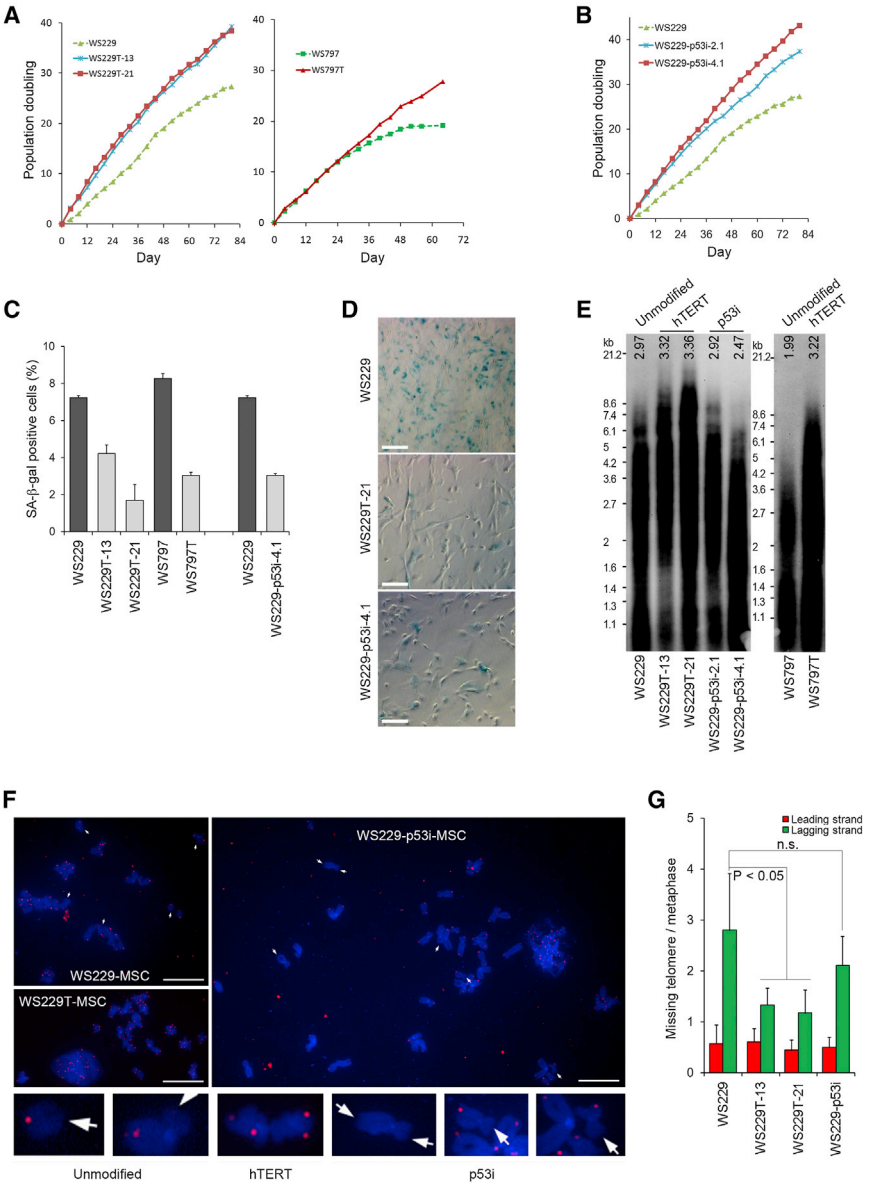

Figure 4. Rescue of Premature Senescence in WS MSCs by Overexpression of hTERT or Knockdown of p53

(A and B) Increased cell proliferation and replicative potential in WS MSCs by overexpression of hTERT (A) or by p53 knockdown (p53i) (B).

(C) The percentage of SA-β-galactosidase-positive cells is reduced by hTERT overexpression or by p53i. Values represent mean of technical replicates ± SD (n = 3).

(D) Representative images of SA-β-galactosidase staining.

(E) WS MSCs expressing hTERT show elongated telomere length compared to unmodified MSC. Telomere length is slightly shortened or unchanged in p53i MSCs.

(F) CO-FISH analysis for the lagging strand telomeres in hTERT-expressing and p53i WS MSCs. Arrows indicate the missing telomeres from the lagging strand.

(G) Quantification of (F). Values represent mean ± SEM (at least 15 metaphase cells were analyzed).

Scale bar, 100 μm (D) or 10 μm (F). See also Figure S4.

telomerase activity is high in embryonic cells, and its activity declines with differentiation (Armstrong et al., 2000; Yang et al., 2008). MSCs and fibroblasts express low telomerase activity, which explains the vulnerability of these cells to replication-induced senescence and telomere dysfunction.

The present study supports the critical role for telomerase in preventing specific lineages of cells from accelerated aging, and it may affect stem cell renewal and their capacity for regeneration (Blasco, 2007). Our observation is consistent with the *Wrn* knockout mouse model, which does not recapitulate the pathogenesis of the disease unless it is expressed on a background of $Terc^{-/-}$ (Chang et al., 2004; Lombard et al., 2000). How telomerase rescues telomere dysfunction is not clear; however, telomerase was reported to extend telomeres and rescue premature aging and reverse tissue degeneration in aged $Terc^{-/-}$ mice with shortened telomeres (Jaskelioff et al., 2011; Samper et al., 2001). An unexpected result from our study is the moderate upregulation of p53 and hence p21 in hTERT-expressing WS cells (Figure S4E). Similar moderate increase of p53 upon hTERT overexpression was also observed in wild-type MSCs (Figure S4H). Shortened telomeres are postulated to activate p53, leading primary cells to senesce (d'Adda di Fagagna et al., 2003). Intriguingly, our data show that hTERT expression in WS MSCs, albeit enhancing their proliferation potential and slowing telomere erosion, increased p53 and

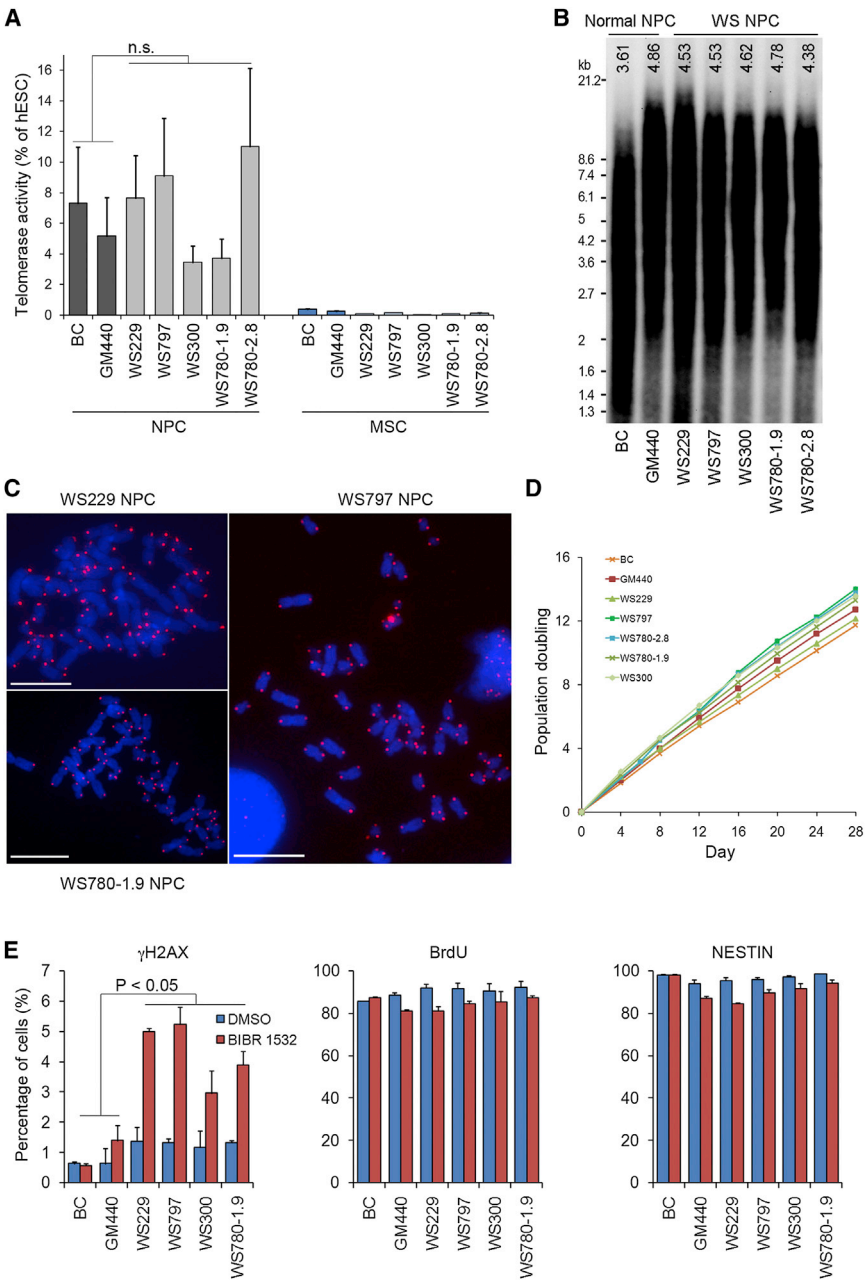

Figure 5. Telomerase Protects and Prevents NPCs from DNA Damage

(A) Comparison of telomerase activity between normal and WS NPCs and MSCs, respectively. The difference between normal and WS NPCs is not significant. Values represent mean of technical replicates ± SD (n = 3).

(B) Telomere length in normal and WS NPCs by TRF Southern blot.

(C) CO-FISH analysis for the lagging strand telomeres in WS NPCs. Few chromosomes show missing telomeres at the lagging strand.

(D) Growth dynamics of NPCs in monolayer culture.

(E) Treatment of telomerase inhibitor BIBR 1532 sensitizes WS NPCs to DNA damage by increasing γH2AX. Active dividing cells and NPC markers were shown by BrdU incorporation (22 hr incubation) and NESTIN expression, respectively. Values represent mean of technical replicates ± SD (n = 3). Scale bar, 10 μm. See also Figure S5.

p21 levels. Consistently, inhibition of telomerase in WS NPCs decreased p53/p21 (Figure S5F). One possible explanation for this phenomenon is that longer telomere repeats stabilize p53 and thus slow their turnover (Milyavsky et al., 2001). However, the detailed mechanism remains to be elucidated.

Telomerase reactivation is a characteristic of successful reprogramming to pluripotency and important for self-renewal in ESCs (Batista et al., 2011; Marion et al., 2009b). We attempted to suppress telomerase activity in WS iPSCs using the same BIBR 1532 concentration in WS-MSC$_{tert}$. However, telomerase is expressed so abundantly in iPSCs that less than 20% of inhibition was achieved. At this level no change in morphology, decrease of SSEA4 (a surface marker for iPSCs), or BrdU incorporation was observed (Figure S1G). Upon differentiation and lineage specification, telomerase is "programmed" to different activity levels, and thus different cells show variable vulnerability to aging. Differential telomerase activity in various stem cells has been documented (Dolci et al., 2002; Morrison et al., 1996; Zimmermann et al., 2003). We compared three different stem cell types: the hESCs

derived from the embryo, the primary MSCs derived from adult bone marrow, and the NPCs derived from the cortical region of human fetal brain for their telomerase activity. The result confirmed a notable difference in telomerase activity among these stem cell types (Figure S2C). In addition to telomerase, the shelterin complex caps and stabilizes the telomeres (Palm and de Lange, 2008). Interestingly, a comparison of shelterin gene expression in the derived normal/WS stem cells indicated a significant difference for some of the capping genes, such as *TRF1*, *TRF2*, and *POT1* (Figure S2B). Coincidently, WRN cooperates with POT1, TRF1, and TRF2 for proper telomere maintenance (Opresko et al., 2002, 2004, 2005). Among them, TRF2 and POT1 are known to repress ATM/ATR cascades in response to uncapping of chromosomal ends (Denchi and de Lange, 2007). *TRF1* is abundantly expressed in pluripotent stem cells and restricted to some other adult stem cells, as *TRF1* is a direct transcriptional target of Oct3/4 (Schneider et al., 2013). These observations suggest that by modulating the telomere-regulating machinery, it is possible to rescue or slow the accelerated aging. Next, targeting the tumor suppressor p53 can mechanically rescue senescence; however, it increases the incidence of tumorigenesis and genomic instability. A major cause in patients with WS is the development of mesenchymal cancers, such as soft tissue sarcoma and osteosarcoma (Chen and Oshima, 2002). It is proposed that immortalization of mesenchymal cancers in WS is acquired by alternative lengthening of the telomere (ALT) instead of telomerase activation (Laud et al., 2005; Multani and Chang, 2007). Although we did not observe immortalization of MSC cultures, our cell model may provide an opportunity to study the unique feature of tumorigenesis in WS. In the present study we focused on stem or progenitors cells; the exhaustion of these progenitors is believed to arise with organismal aging. Terminally differentiated cells, such as fibroblasts, bone cells, and endothelial and smooth muscle cells, as contrasted to neurons, may provide more insight into the underlying mechanism of accelerated aging.

EXPERIMENTAL PROCEDURES

Cell Lines and Cultures

We obtained WS and normal control fibroblasts from Coriell Cell Repositories. Additional normal control fibroblasts (BC, AN1, AN2, and AN3) were obtained from healthy donors at the Clinical Center of National Institutes Health with written consent. hESC lines CT2 and ESI-053 were obtained from University of Connecticut Stem Cell Core and BioTime, respectively. Bone marrow MSCs (BM-MSCs) and ReNcell CX human NPCs (CX-NPCs) were purchased from StemCell Technologies and Millipore, respectively. All cell cultures were maintained as suggested by the suppliers.

Generation and Characterization of iPSCs

We reprogrammed WS fibroblasts with high-titer polycistronic lentivirus-expressing human OCT4, SOX2, KLF4, and c-MYC (hSTEMCCA) (Somers et al., 2010). Four days after transduction, cells were transferred to MEF feeders in iPSC culture medium supplemented with HDAC and TGF-β RI kinase inhibitors (Millipore, cat. no. CS204423, CS204420) for 12 days. WS iPSC colonies started to appear 2 weeks after transduction. Colonies were picked from day 30 to 40 and expanded on MEF feeders in hESC medium containing 80% KO Dulbecco's modified Eagle's medium (DMEM), 20% KSR, 1% nonessential amino acids, 1% GlutaMAX, 0.1 mM β-mercaptoethanol, and 10 ng/ml bFGF. iPSCs were characterized by expression of pluripotency markers NANOG, SOX2, OCT4, SSEA3, SSEA4, TRA1-60, and TRA1-81 using immunofluorescence staining. iPSC pluripotency was tested by injecting cells into SCID mice at the kidney and testis capsules and harvested for histologic analysis (Applied Stem Cells). Karyotyping was performed by the WiCell Cytogenetics Lab. To generate telomerized and p53 knockdown cells, we transduced WS fibroblasts with retrovirus-expressing hTERT (Addgene plasmid 1773) or p53 shRNA (Santa Cruz) and selected by 100 μg/ml hygromycin B or 1 μg/ml puromycin. Stable cultures were reprogrammed by hSTEMCCA as described above.

Differentiation and Characterization of MSCs Derived from iPSCs

To derive MSCs, we trypsinized iPSCs to single cells and plated them on a gelatin-coated dish in MSC differentiation medium containing 20% of MSC-qualified FBS (Life Technologies), 10 ng/ml of bFGF, PDGF AB, and EGF (all Peprotech) in alpha MEM (Lian et al., 2010). Differentiating cells were split by trypsin for 3–4 times when becoming confluent. After 2 weeks, cells were sorted for $CD105^+$/$CD90^+$/$CD24^-$ using fluorescence-activated cell sorting (FACS) Aria (BD Biosciences). Sorted cells were allowed to grow for 3–4 days and subsequently plated on a plastic dish at 1×10^4 cells/cm^2 in MSC medium containing 10% MSC-qualified FBS, 5 ng/ml bFGF in low-glucose DMEM. MSCs were split every 4 days, and a growth curve was constructed by direct cell counting at each passage. For characterization of MSCs, we analyzed expression of MSC phenotype ($CD73^+$, $CD90^+$, $CD105^+$, $CD44^+$, $CD166^+$, $CD29^+$, $CD34^-$, $CD45^-$, $CD14^-$, $CD19^-$, and HLA-DR^-) by flow cytometry. All antibodies and control immunoglobulin G isotypes were purchased from BD Biosciences. BM-MSCs were included as a positive control. To test multipotency, we differentiated MSCs to adipocytes, osteocytes, and chondrocytes by STEMPRO Adipogenesis, Osteogenesis, and Chondrogenesis Differentiation Media (Life Technologies). Adipocytes and osteocytes were stained with Nile Red and Alizarin Red S after 4 and 2 weeks of differentiation, respectively. Cell aggregates of chondrocytes were fixed and sectioned for Safranin O staining after 2 weeks of differentiation.

Differentiation and Characterization of NPCs Derived from iPSCs

To derived NPCs, we formed embryoid bodies (EBs) from iPSCs cultured on Matrigel with mTeSR1 medium (StemCell Technologies) on AggreWell (Marchetto et al., 2010). EBs were induced for

neural differentiation by STEMdiff Neural Induction Medium (StemCell Technologies) for 5 days on AggreWell and then transferred to poly-L-ornithine (PLO)/laminin-coated plates for another 7 days. Neural rosettes were collected by treating cell aggregates with Neural Rosette Selection Reagent and then were replated on PLO/laminin-coated plate. NPCs were allowed to grow to confluence from neural rosettes and thereafter passed every 4 days. NPCs were cultured as monolayer on PLO/laminin-coated plates in N2B27 medium containing 0.5% N2, 1% B27, EGF, and bFGF (20 ng/ml of each) in DMEM/F12 with GlutaMAX (Life Technologies). For characterization of NPCs, we analyzed expression of neural stem markers NESTIN (Millipore) and SOX1 (BD Biosciences) by immunofluorescence staining. To test multipotency, we plated NPCs on Matrigel-coated plates and cultured them in N2B27 medium with the withdrawal of EGF and bFGF and inclusion of neurotrophic factors BDNF, CNTF, GDNF, and IGF1 (10 ng/ml of each) (Peprotech) and 1 μM of cAMP (Wang et al., 2013). After 2 weeks of differentiation, cells were examined for the expression of neuronal markers TUJ1, MAP2, and DCX and the astrocyte marker GFAP by immunofluorescence staining.

Telomerase Activity Assay by TRAP

We measure telomerase activity by TRAP assay (Wright et al., 1995) using the TRAPeze RT Telomerase Detection Kit (Millipore). Crude protein lysate was extracted and adjusted to 0.5 μg/μl. Lysate (1 μg) was incubated with the TRAPeze RT reaction mix at 30°C for 30 min. The telomerase product was amplified by real-time PCR using hot-start Taq polymerase with the inclusion of a TSR8 standard curve. Telomerase activity was normalized by the TSK and expressed as the relative level to hESCs. All TRAP assays were performed as three independent technical replicates.

Southern Blot Analysis of Terminal Restriction Fragment Lengths

Telomere length was determined as previously described (Kimura et al., 2010). Genomic DNA was digested with RsaI and HinfI overnight and resolved in 0.6% agarose gel. DNA was transferred to nylon membrane (Ambion) by capillary method overnight. Membrane was hybridized to DIG-labeled telomere probe $(CCCTAA)_3$ at 42°C overnight. After stringent wash (0.1% SDS in 2X SSC), membrane was blocked and incubated with anti-DIG-AP antibodies for half an hour at room temperature. Terminal restriction fragment (TRF) was measured by the intensity of the AP substrates using chemiluminescence detection. All reagents were from the Telo TAGGG Telomere Length Assay Kit (Roche). Average TRF length was calculated by mean TRF length = $\Sigma (OD_i) / \Sigma (OD_i/MW_i)$, where OD is the optical density at position i and MWi is the TRF length at that position.

Telomere CO-FISH

Telomere CO-FISH was performed as previously described, with minor modifications (Crabbe et al., 2004). Briefly, dividing cells were incorporated with 7.5 mM BrdU and 2.5 mM BrdC for approximately 1 doubling time (21 hr for iPSCs, 26–35 hr for MSCs, and 30 hr for NPCs). Metaphases cells were enriched by treatment of Colcemid for 4–8 hr and fixed with fresh methanol and glacial acetic acid (3:1) at 4°C overnight. Cells were washed and dropped on HCl-treated glass slides. To remove newly synthesized BrdU/BrdC-incorporated DNA strands, cells were stained with 0.5 μg/ml Hoechst 33258, exposed to UV light for half an hour, and then digested by Exonuclease III (10 U/μl) for 10 min at room temperature. Hybridization was performed using fluorescence-labeled PNA telomere probes (PNA Bio) for the leading stand $(TTAGGG)_3$ and lagging strand $(CCCTAA)_3$, sequentially hybridized at room temperature for 2 hr. Slides were washed twice in 70% formamide at room temperature followed by three washes in 0.2× SSC at 57°C. Slides were stained with DAPI and visualized in Aviovert 200 Inverted Fluorescent Microscope (Zeiss) using the 100× oil lens. A total number of 15–20 metaphases per sample were analyzed and represented as mean ± SEM.

SA-β-Galactosidase Assay

We detected cell senescence by SA-β-gal cytochemical staining (Sigma-Aldrich). Adherent cells on the culture dish were fixed with 2% formaldehyde and 0.2% glutaraldehyde for 6 min and stained with staining solution containing 5 mM potassium ferricyanide, 5 mM potassium ferrocyanide, and 1 mg/ml X-gal at pH 6 overnight. Alternatively, SA-β-gal activity was measured by fluorescence substrates (Debacq-Chainiaux et al., 2009). We treated cells with 100 nM of lysosomal inhibitory drug Bafilomycin A1 (Sigma-Aldrich) for 1 hr. Then a β-gal substrate C_{12}FDG (Life Technologies) that becomes fluorescent after enzymatic cleavage was incubated at a final concentration of 33 μM for 2 hr. Cells were washed and trypsinized for FACS analysis. Fibroblast culture of low passage number was included as negative control for senescence. All experiments were performed in triplicate wells and represented as mean ± SD.

BrdU Incorporation and Flow Cytometry

To measure DNA synthesis at S phase, we incubated actively diving cells with 10 μM BrdU for 45 min (iPSCs) or 2 hr (MSCs/NPCs). Cells were fixed, permeabilized, and treated with DNase I and then incubated with fluorescein-isothiocyanate-labeled anti-BrdU antibodies (BD Biosciences). iPSCs were costained with SSEA4, and NPCs were costained with NESTIN for gating of undifferentiated cells. DNA content was stained by 7-AAD. Cells were washed and analyzed by FACSAria (BD Biosciences). To measure cell proliferation and DNA damage in NPCs with BIBR 1532 treatment, we labeled cells with BrdU for 22 hr and incubated cells with Alexa Fluor 647-labeled anti-γH2AX (pS139) (BD Biosciences). All experiments were performed in triplicate wells and represented as mean ± SD.

Microarray Analysis and Bioinformatics

We profiled gene expression by GeneChip Human Gene 1.0 ST Array (Affymetrix). Total RNA (100 ng) was converted to cRNA by in vitro transcription of the T7-tagged cDNA using the Ambion WT Expression Kit (Ambion). cRNA (10 μg) was converted to fragmented and labeled cDNA probes using the WT Terminal Labeling and Control Kit (Affymetrix). cDNA probes were hybridized to the chips overnight at 45°C and stained at the GeneChip Fluidics Station 450. Signals were scanned by GeneChip Scanner 3000 7G. Microarray data were analyzed by Partek Genomics Suite 6.6

with quantile normalization and RMA background correction. Transcriptome profiles were compared using principal component analysis (PCA) and unsupervised hierarchical clustering of all genes by comparing the sample dissimilarity using Pearson correlation. To analyze differentially expressed genes in WS fibroblasts, we removed a batch effect due to scan date and compared the difference of the genes by one-way ANOVA. We clustered the iPSC/hESC and fibroblast samples based on the differentially expressed gene sets. Genes with a fold change >2 or <−2 and p value <0.05 with a false discovery rate (FDR) <0.05 were submitted for gene ontology analysis based on the category of biological function. All microarray array experiments were repeated as duplicate experiments for each sample.

Western Blot Analysis

Western blot analysis was performed as previously described (Cheung et al., 2011). Primary antibodies used include anti-WRN (Sigma-Aldrich, clone 195C), anti-γH2AX (Ser139) (Millipore, clone JBW301), anti-p53 (Santa Cruz Biotech, sc-126), anti-α-actinin (Santa Cruz Biotech, sc-17829), anti-p16 (Santa Cruz Biotech, sc-468), anti-p21 (Cell Signaling, #2946), anti-phospho-ATM (S1981) (Abcam, clone EP1890Y), anti-53BP1 (Santa Cruz Biotech, sc-22760), and anti-phospho-p53 (Ser15) (Cell Signaling, #9284).

Statistical Analysis

All comparisons between normal and WS samples were tested by unpaired, two-tailed Student's t test. A p value <0.05 was considered statistically significant.

ACCESSION NUMBERS

Microarray data have been deposited in the National Center for Biotechnology Information Gene Expression Omnibus database under the accession ID GSE48761.

SUPPLEMENTAL INFORMATION

Supplemental Information includes five figures and two tables and can be found with this article online at http://dx.doi.org/10.1016/j.stemcr.2014.02.006.

ACKNOWLEDGMENTS

We thank Dr. Bob Weinberg for providing the pBABE-hygro-hTERT retroviral vector. This research was supported by an intramural research grant from the Eunice Kennedy Shriver National Institute of Child Health and Human Development.

Received: August 21, 2013
Revised: February 20, 2014
Accepted: February 20, 2014
Published: March 27, 2014

REFERENCES

Abdallah, P., Luciano, P., Runge, K.W., Lisby, M., Géli, V., Gilson, E., and Teixeira, M.T. (2009). A two-step model for senescence triggered by a single critically short telomere. Nat. Cell Biol. *11*, 988–993.

Armstrong, L., Lako, M., Lincoln, J., Cairns, P.M., and Hole, N. (2000). mTert expression correlates with telomerase activity during the differentiation of murine embryonic stem cells. Mech. Dev. *97*, 109–116.

Banito, A., Rashid, S.T., Acosta, J.C., Li, S., Pereira, C.F., Geti, I., Pinho, S., Silva, J.C., Azuara, V., Walsh, M., et al. (2009). Senescence impairs successful reprogramming to pluripotent stem cells. Genes Dev. *23*, 2134–2139.

Batista, L.F., Pech, M.F., Zhong, F.L., Nguyen, H.N., Xie, K.T., Zaug, A.J., Crary, S.M., Choi, J., Sebastiano, V., Cherry, A., et al. (2011). Telomere shortening and loss of self-renewal in dyskeratosis congenita induced pluripotent stem cells. Nature *474*, 399–402.

Blasco, M.A. (2007). Telomere length, stem cells and aging. Nat. Chem. Biol. *3*, 640–649.

Brosh, R.M., Jr., von Kobbe, C., Sommers, J.A., Karmakar, P., Opresko, P.L., Piotrowski, J., Dianova, I., Dianov, G.L., and Bohr, V.A. (2001). Werner syndrome protein interacts with human flap endonuclease 1 and stimulates its cleavage activity. EMBO J. *20*, 5791–5801.

Chang, S., Multani, A.S., Cabrera, N.G., Naylor, M.L., Laud, P., Lombard, D., Pathak, S., Guarente, L., and DePinho, R.A. (2004). Essential role of limiting telomeres in the pathogenesis of Werner syndrome. Nat. Genet. *36*, 877–882.

Chen, L., and Oshima, J. (2002). Werner syndrome. J. Biomed. Biotechnol. *2*, 46–54.

Chen, L., Lee, L., Kudlow, B.A., Dos Santos, H.G., Sletvold, O., Shafeghati, Y., Botha, E.G., Garg, A., Hanson, N.B., Martin, G.M., et al. (2003). LMNA mutations in atypical Werner's syndrome. Lancet *362*, 440–445.

Cheung, H.H., Davis, A.J., Lee, T.L., Pang, A.L., Nagrani, S., Rennert, O.M., and Chan, W.Y. (2011). Methylation of an intronic region regulates miR-199a in testicular tumor malignancy. Oncogene *30*, 3404–3415.

Crabbe, L., Verdun, R.E., Haggblom, C.I., and Karlseder, J. (2004). Defective telomere lagging strand synthesis in cells lacking WRN helicase activity. Science *306*, 1951–1953.

Crabbe, L., Jauch, A., Naeger, C.M., Holtgreve-Grez, H., and Karlseder, J. (2007). Telomere dysfunction as a cause of genomic instability in Werner syndrome. Proc. Natl. Acad. Sci. USA *104*, 2205–2210.

d'Adda di Fagagna, F., Reaper, P.M., Clay-Farrace, L., Fiegler, H., Carr, P., Von Zglinicki, T., Saretzki, G., Carter, N.P., and Jackson, S.P. (2003). A DNA damage checkpoint response in telomere-initiated senescence. Nature *426*, 194–198.

Debacq-Chainiaux, F., Erusalimsky, J.D., Campisi, J., and Toussaint, O. (2009). Protocols to detect senescence-associated beta-galactosidase (SA-betagal) activity, a biomarker of senescent cells in culture and in vivo. Nat. Protoc. *4*, 1798–1806.

Denchi, E.L., and de Lange, T. (2007). Protection of telomeres through independent control of ATM and ATR by TRF2 and POT1. Nature *448*, 1068–1071.

Dolci, S., Levati, L., Pellegrini, M., Faraoni, I., Graziani, G., Di Carlo, A., and Geremia, R. (2002). Stem cell factor activates telomerase in mouse mitotic spermatogonia and in primordial germ cells. J. Cell Sci. *115*, 1643–1649.

Goto, M., Ishikawa, Y., Sugimoto, M., and Furuichi, Y. (2013). Werner syndrome: a changing pattern of clinical manifestations in Japan (1917∼2008). Bioscience trends *7*, 13–22.

Ishikawa, N., Nakamura, K., Izumiyama-Shimomura, N., Aida, J., Ishii, A., Goto, M., Ishikawa, Y., Asaka, R., Matsuura, M., Hatamochi, A., et al. (2011). Accelerated in vivo epidermal telomere loss in Werner syndrome. Aging (Albany, N.Y. Online) *3*, 417–429.

Jaskelioff, M., Muller, F.L., Paik, J.H., Thomas, E., Jiang, S., Adams, A.C., Sahin, E., Kost-Alimova, M., Protopopov, A., Cadiñanos, J., et al. (2011). Telomerase reactivation reverses tissue degeneration in aged telomerase-deficient mice. Nature *469*, 102–106.

Kawamura, T., Suzuki, J., Wang, Y.V., Menendez, S., Morera, L.B., Raya, A., Wahl, G.M., and Izpisúa Belmonte, J.C. (2009). Linking the p53 tumour suppressor pathway to somatic cell reprogramming. Nature *460*, 1140–1144.

Kimura, M., Stone, R.C., Hunt, S.C., Skurnick, J., Lu, X., Cao, X., Harley, C.B., and Aviv, A. (2010). Measurement of telomere length by the Southern blot analysis of terminal restriction fragment lengths. Nat. Protoc. *5*, 1596–1607.

Lapasset, L., Milhavet, O., Prieur, A., Besnard, E., Babled, A., Aït-Hamou, N., Leschik, J., Pellestor, F., Ramirez, J.M., De Vos, J., et al. (2011). Rejuvenating senescent and centenarian human cells by reprogramming through the pluripotent state. Genes Dev. *25*, 2248–2253.

Laud, P.R., Multani, A.S., Bailey, S.M., Wu, L., Ma, J., Kingsley, C., Lebel, M., Pathak, S., DePinho, R.A., and Chang, S. (2005). Elevated telomere-telomere recombination in WRN-deficient, telomere dysfunctional cells promotes escape from senescence and engagement of the ALT pathway. Genes Dev. *19*, 2560–2570.

Li, B., and Comai, L. (2001). Requirements for the nucleolytic processing of DNA ends by the Werner syndrome protein-Ku70/80 complex. J. Biol. Chem. *276*, 9896–9902.

Lian, Q., Zhang, Y., Zhang, J., Zhang, H.K., Wu, X., Zhang, Y., Lam, F.F., Kang, S., Xia, J.C., Lai, W.H., et al. (2010). Functional mesenchymal stem cells derived from human induced pluripotent stem cells attenuate limb ischemia in mice. Circulation *121*, 1113–1123.

Liu, G.H., Barkho, B.Z., Ruiz, S., Diep, D., Qu, J., Yang, S.L., Panopoulos, A.D., Suzuki, K., Kurian, L., Walsh, C., et al. (2011). Recapitulation of premature ageing with iPSCs from Hutchinson-Gilford progeria syndrome. Nature *472*, 221–225.

Lombard, D.B., Beard, C., Johnson, B., Marciniak, R.A., Dausman, J., Bronson, R., Buhlmann, J.E., Lipman, R., Curry, R., Sharpe, A., et al. (2000). Mutations in the WRN gene in mice accelerate mortality in a p53-null background. Mol. Cell. Biol. *20*, 3286–3291.

Lu, W., Zhang, Y., Liu, D., Songyang, Z., and Wan, M. (2013). Telomeres-structure, function, and regulation. Exp. Cell Res. *319*, 133–141.

Marchetto, M.C., Carromeu, C., Acab, A., Yu, D., Yeo, G.W., Mu, Y., Chen, G., Gage, F.H., and Muotri, A.R. (2010). A model for neural development and treatment of Rett syndrome using human induced pluripotent stem cells. Cell *143*, 527–539.

Marión, R.M., Strati, K., Li, H., Murga, M., Blanco, R., Ortega, S., Fernandez-Capetillo, O., Serrano, M., and Blasco, M.A. (2009a). A p53-mediated DNA damage response limits reprogramming to ensure iPS cell genomic integrity. Nature *460*, 1149–1153.

Marion, R.M., Strati, K., Li, H., Tejera, A., Schoeftner, S., Ortega, S., Serrano, M., and Blasco, M.A. (2009b). Telomeres acquire embryonic stem cell characteristics in induced pluripotent stem cells. Cell Stem Cell *4*, 141–154.

Milyavsky, M., Mimran, A., Senderovich, S., Zurer, I., Erez, N., Shats, I., Goldfinger, N., Cohen, I., and Rotter, V. (2001). Activation of p53 protein by telomeric (TTAGGG)n repeats. Nucleic Acids Res. *29*, 5207–5215.

Mori, H., Tomiyama, T., Maeda, N., Ozawa, K., and Wakasa, K. (2003). Lack of amyloid plaque formation in the central nervous system of a patient with Werner syndrome. Neuropathology *23*, 51–56.

Morrison, S.J., Prowse, K.R., Ho, P., and Weissman, I.L. (1996). Telomerase activity in hematopoietic cells is associated with self-renewal potential. Immunity *5*, 207–216.

Muftuoglu, M., Oshima, J., von Kobbe, C., Cheng, W.H., Leistritz, D.F., and Bohr, V.A. (2008). The clinical characteristics of Werner syndrome: molecular and biochemical diagnosis. Hum. Genet. *124*, 369–377.

Multani, A.S., and Chang, S. (2007). WRN at telomeres: implications for aging and cancer. J. Cell Sci. *120*, 713–721.

Opresko, P.L., von Kobbe, C., Laine, J.P., Harrigan, J., Hickson, I.D., and Bohr, V.A. (2002). Telomere-binding protein TRF2 binds to and stimulates the Werner and Bloom syndrome helicases. J. Biol. Chem. *277*, 41110–41119.

Opresko, P.L., Otterlei, M., Graakjaer, J., Bruheim, P., Dawut, L., Kølvraa, S., May, A., Seidman, M.M., and Bohr, V.A. (2004). The Werner syndrome helicase and exonuclease cooperate to resolve telomeric D loops in a manner regulated by TRF1 and TRF2. Mol. Cell *14*, 763–774.

Opresko, P.L., Mason, P.A., Podell, E.R., Lei, M., Hickson, I.D., Cech, T.R., and Bohr, V.A. (2005). POT1 stimulates RecQ helicases WRN and BLM to unwind telomeric DNA substrates. J. Biol. Chem. *280*, 32069–32080.

Palm, W., and de Lange, T. (2008). How shelterin protects mammalian telomeres. Annu. Rev. Genet. *42*, 301–334.

Rossi, M.L., Ghosh, A.K., and Bohr, V.A. (2010). Roles of Werner syndrome protein in protection of genome integrity. DNA Repair (Amst.) *9*, 331–344.

Samper, E., Flores, J.M., and Blasco, M.A. (2001). Restoration of telomerase activity rescues chromosomal instability and premature aging in Terc-/- mice with short telomeres. EMBO Rep. *2*, 800–807.

Schneider, R.P., Garrobo, I., Foronda, M., Palacios, J.A., Marion, R.M., Flores, I., Ortega, S., and Blasco, M.A. (2013). TRF1 is a stem cell marker and is essential for the generation of induced pluripotent stem cells. Nature communications *4*, 1946.

Schulz, V.P., Zakian, V.A., Ogburn, C.E., McKay, J., Jarzebowicz, A.A., Edland, S.D., and Martin, G.M. (1996). Accelerated loss of telomeric repeats may not explain accelerated replicative decline of Werner syndrome cells. Hum. Genet. *97*, 750–754.

Somers, A., Jean, J.C., Sommer, C.A., Omari, A., Ford, C.C., Mills, J.A., Ying, L., Sommer, A.G., Jean, J.M., Smith, B.W., et al. (2010). Generation of transgene-free lung disease-specific human induced pluripotent stem cells using a single excisable lentiviral stem cell cassette. Stem Cells *28*, 1728–1740.

Taboski, M.A., Sealey, D.C., Dorrens, J., Tayade, C., Betts, D.H., and Harrington, L. (2012). Long telomeres bypass the requirement for telomere maintenance in human tumorigenesis. Cell reports *1*, 91–98.

Takai, H., Smogorzewska, A., and de Lange, T. (2003). DNA damage foci at dysfunctional telomeres. Current biology: CB *13*, 1549–1556.

Wang, L., Wang, L., Huang, W., Su, H., Xue, Y., Su, Z., Liao, B., Wang, H., Bao, X., Qin, D., et al. (2013). Generation of integration-free neural progenitor cells from cells in human urine. Nat. Methods *10*, 84–89.

Wright, W.E., Shay, J.W., and Piatyszek, M.A. (1995). Modifications of a telomeric repeat amplification protocol (TRAP) result in increased reliability, linearity and sensitivity. Nucleic Acids Res. *23*, 3794–3795.

Yang, C., Przyborski, S., Cooke, M.J., Zhang, X., Stewart, R., Anyfantis, G., Atkinson, S.P., Saretzki, G., Armstrong, L., and Lako, M. (2008). A key role for telomerase reverse transcriptase unit in modulating human embryonic stem cell proliferation, cell cycle dynamics, and in vitro differentiation. Stem Cells *26*, 850–863.

Zhang, J., Lian, Q., Zhu, G., Zhou, F., Sui, L., Tan, C., Mutalif, R.A., Navasankari, R., Zhang, Y., Tse, H.F., et al. (2011). A human iPSC model of Hutchinson Gilford Progeria reveals vascular smooth muscle and mesenchymal stem cell defects. Cell Stem Cell *8*, 31–45.

Zimmermann, S., Voss, M., Kaiser, S., Kapp, U., Waller, C.F., and Martens, U.M. (2003). Lack of telomerase activity in human mesenchymal stem cells. Leukemia *17*, 1146–1149.